Inorg. Chem. **2005**, *44*, 955–963

Di([5]trovacenyl)ethyne, Di([5]trovacenyl)butadiyne, and Di-1,4-([5]trovacenylethynyl)benzene: Electrocommunication and Magnetocommunication Mediated by —C≡C—, —C≡C—C≡C— and —C≡C—C_6H_4—C≡C— Spacers†

Christoph Elschenbroich,* Jörn Plackmeyer, Mathias Nowotny, Klaus Harms, Jürgen Pebler, and Olaf Burghaus

Fachbereich Chemie, Philipps-Universität, D-35032 Marburg, Germany

Received July 19, 2004

The synthesis of dinuclear derivatives of trovacene (η^7-C_7H_7)V(η^5-C_5H_5) (**1•**) is reported, in which ethynyl (**6••**), butadiynyl (**7••**), and 1,4-di(ethynyl)phenyl (**8••**) groups serve as spacers between paramagnetic ($S = {}^1/_2$) [5]trovacenyl units. The mononuclear precursors [5]trovacenylcarbaldehyde (**2•**) and [5]trovacenylacetylene (**4•**) are also described. Structural characterization by X-ray diffraction has been performed for **4•**, **6••**, **7••**, and **8••**. Electronic communication as gleaned from cyclic voltammetry only manifests itself in the reduction processes where redox splitting $\delta E_{1/2}$(0/1–, 1–/2–) is resolved for **6••** ($\delta E_{1/2} = 150$ mV) and indicated for **7••** ($\delta E_{1/2} \lesssim 80$ mV). Magnetocommunication leads to exchange coupling of the two electron spins which reside in vanadium centered orbitals. The values J_{EPR}(**6••**) = (–)0.92, J_{EPR}(**7••**) = (–)0.56, and J_{EPR}(**8••**) = (–)0.005 cm^{-1} are derived from the ^{51}V hyperfine patterns. Accordingly, attenuation of exchange interaction by oligoalkyne spacers is weak, corresponding to a factor of 0.6 only per added —C≡C— unit. In the determination of very weak long distance exchange interactions, EPR excels because of the range $5 \times 10^{-4} \lesssim J \lesssim 1.5$ cm^{-1} accessible in the case of ^{51}V as a reporting magnetic nucleus and because competing intermolecular exchange is quenched in dilute fluid solution. This is demonstrated by the value J_χ(**7••**) = –3.84 cm^{-1} obtained from a magnetic susceptibility study, which exceeds J_{EPR}(**7••**) by a factor of 7. The small magnitude of spin exchange interaction between trovacene units reflects the fact that the spin bearing V3d_{z^2} orbital is virtually orthogonal to the π-perimeter ligand orbitals and weakly overlapping only with the $a_{1g}(\sigma)$ ring orbitals, creating two bottlenecks for spin-exchange in the spacer-containing ditrovacenes.

Introduction

Justification for the intensive study of binuclear complexes which feature oligoalkyne spacers derives from their potential use as "carbon rods", "molecular wires", or, ultimately, "electronic devices". Elaborations of these concepts and numerous references may be found in papers by Lapinte,[1] Bruce,[2] Gladysz,[3] Ziessel,[4] Hong,[5] Gleiter,[6] and Ren.[7] An asset of oligoethynylene, OE, and oligo(phenylene ethynylene), OPE, spacers is their rigidity which provides controllable distance between interacting terminal units. The ability of the spacer —$(C{\equiv}C)_n$— to transmit electronic effects has commonly been studied by electrochemistry, using the redox−splitting $\delta E_{1/2}$, i.e., the potential difference of consecutive redox steps as a measure of intramolecular intermetallic communication. In cases where $\delta E_{1/2}$ is sufficiently large to allow generation of a mixed valence species, observation of an MMCT (intervalence) band in the NIR also attests to electron mediating properties of the spacers.

* To whom correspondence should be addressed. E-mail: eb@chemie.uni-marburg.de.

† Trovacene Chemistry. 9. Part 8: Schiemann, O.; Plackmeyer, J.; Fritscher, J.; Pebler, J.; Elschenbroich, Ch. *Appl. Magn. Reson*. **2004**, *26*, 171.

(1) (a) Paul, F.; Lapinte, C. *Coord. Chem. Rev*. **1998**, *178−180*, 431. (b) Paul, F.; Lapinte, C. *Unusual Structures and Physical Porperties in Organometallic Chemistry*; Gielen, M., Willem, R., Wrackmeyer, B., Eds.; Wiley: West Sussex, U.K., 2002; Chapter 6.

(2) (a) Bruce, M. I.; Ellis, B. G.; Low, P. J.; Skelton, B. W.; White, A. H. *Organometallics* **2003**, *22*, 3184. (b) Low, P. J.; Bruce, M. I. *Adv. Organomet. Chem*. **2001**, *48*, 71. (c) Low, P. J.; Bruce, M. I. *Adv. Organomet. Chem*. **2004**, *50*, 179.

(3) Mohr, W.; Stahl, J.; Hampel, F.; Gladysz, J. A. *Chem. Eur. J*. **2003**, *9*, 3324.

(4) Grosshenny, V.; Harriman, A.; Ziessel, R. *Angew. Chem., Int. Ed. Engl*. **1995**, *34*, 2921.

(5) Hong, B. *Comments Inorg. Chem*. **1999**, *20*, 177.

(6) Classen, J.; Gleiter, R.; Rominger, F. *Eur. J. Inorg. Chem*. **2002**, 2040.

(7) Xu, G.-L.; Zon, G.; Ni, Y.-H.; DeRosa, M. C.; Crutchley, R. J.; Ren, T. *J. Am. Chem. Soc*. **2003**, *125*, 10057.

10.1021/ic040090z CCC: $30.25
Published on Web 01/15/2005

With increasing intermetallic distance and/or diminishing transfer abilities of the spacer, more sensitive detection methods must be applied. If the terminal groups at the $-(C\equiv C)_n-$ chain are paramagnetic, determination of the exchange coupling constant J provides the information. This can be accomplished by magnetic susceptometry for $J \gtrsim 1$ cm^{-1} and by EPR spectroscopy for much smaller J values, the limit being set by the magnitude of electron−nuclear hyperfine interaction with the respective magnetic nucleus present. For (η^7-C_7H_7)V(η^5-C_5H_5) (trovacene, TVC, **1**$^\bullet$), the isotropic hyperfine coupling constant amounts to $a(^{51}V, \mathbf{1}^\bullet) = -6.98$ mT (6.5×10^{-3} cm^{-1}), which permits the exchange coupling constant J to be derived from the ^{51}V hyperfine pattern in the range $5 \times 10^{-4} \lesssim J < 1.5$ cm^{-1}, i.e., the regime of weak coupling. Thus, in the study of V^0 sandwich complexes EPR and susceptometry are complementary. In the following, we report on the preparation of the species [5]TVC−$(C\equiv C)_n$−[5]TVC ($n = 1, 2$), and their structural, electrochemical, and magnetic properties.

Alkyne- and oligoalkyne spacered bimetallocenes (η^5-C_5H_5)M(η^5-C_5H_4−$(C\equiv C)_n$−η^5-C_5H_4)M(η^5-C_5H_5), partially in ring-methylated form, have been prepared previously (M = Fe,[8a−c] M = Ni[8b]) and studied by a variety of methods. Yet, exchange coupling between two paramagnetic metallocenes, mediated by an alkyne spacer, has been addressed only once for the case of the diradical dication [$CpFeC_5H_4$−C≡C−C_5H_4-FeCp]$^{+\bullet+\bullet}$.[9a] The result, $J = -3.1$ cm^{-1}, obtained from a magnetic susceptibility/temperature plot, was regarded as an order of magnitude estimate only, because the ferrocenium ion features an orbitally degenerate $^2E_{2g}$ state whose orbital magnetism is not accounted for in the Bleaney−Bowers function used for fitting the data. Spin exchange propagated by a $-(C\equiv C)_2-$ bridge has been studied for a biradical containing terminal iminoxyl groups. Fast exchange on the ^{14}N hyperfine time scale applies here since the EPR spectrum exhibits a quintet (1:2:3:2:1) with the splitting $a(^{14}N)/2$ (monoradical).[9b] No determination of J by means of magnetic susceptometry has been forthcoming, though.

While the study of intramolecular communication in biradicals by means of EPR is a valuable goal in itself, the question must be addressed whether the more important phenomena of intramolecular long-distance electron transfer and energy transfer are somehow related to electron-spin exchange-coupling, bearing in mind that ET is a one-electron process, whereas exchange coupling is a two-electron process. In fact, as Forbes[10] has pointed out, both processes are facets of the more general donor−acceptor interaction having in common the electron transfer matrix element V. Distance dependence of the latter is profitably studied by means of exchange coupling J since contributions from the reorganization energies λ_{out} and λ_{in} need not be considered. λ_{out} is negligible because the biradicals studied are neutral species and intramolecular exchange does not involve changes in polarity. λ_{in} is vanishingly small due to the fact that in the probe TV̇C the SOMO, which engages in coupling, is a metal centered, nonbonding orbital. These simple arguments, which are based on spin delocalization, regard spin−spin coupling as a consequence of double exchange such that both unpaired electrons adopt an excited configuration and populate the LUMO of the bridge where they couple antiferromagnetically, in line with the Pauli principle. Admittedly, finding a conceptual link between the part of exchange coupling J which stems from spin polarization of the spacer bonds and intramolecular electron and energy transfer will be somewhat more involved. Here, describing spin polarization by means of configuration interaction supplies a way to take the nature of the spacer molecular orbitals into account explicitly.

Results and Discussion

Synthesis. The target compounds ([5]trovacenyl)ethyne (**4**$^\bullet$), (di([5]trovacenyl)ethyne (**6**$^{\bullet\bullet}$), di([5]trovacenyl)butadiyne (**7**$^{\bullet\bullet}$), and di-1,4-([5]trovacenyl ethynyl)benzene (**8**$^{\bullet\bullet}$) were prepared according to the reaction sequences shown in Scheme 1. Sonogashira coupling (c) yielded a mixture of **6**$^{\bullet\bullet}$ and **7**$^{\bullet\bullet}$, from which only compound **7**$^{\bullet\bullet}$, the product resulting from initial H/I exchange at **4**$^\bullet$, could be isolated pure by means of repeated crystallization. Therefore, in order to prepare pure **6**$^{\bullet\bullet}$, recourse was taken to use Stille coupling (b). Negishi coupling (d) posed no problems in that homocoupling proved to be absent.

Structural Study. Drawings of the structures of **6**$^{\bullet\bullet}$, **7**$^{\bullet\bullet}$, and **8**$^{\bullet\bullet}$, determined by X-ray diffraction, are depicted in Figure 1; pertinent distances are given in the caption. Interestingly, the monoalkyne **6**$^{\bullet\bullet}$ and the 1,4-dialkynylbenzene derivative **8**$^{\bullet\bullet}$ in the crystal adopt antiperiplanar conformations with parallel sandwich axes whereas the dialkyne **7**$^{\bullet\bullet}$, unlike the ferrocene analogue,[8c] is encountered in a twisted conformation, the sandwich axes being inclined at 90°. A simplified packing diagram for compound **7**$^{\bullet\bullet}$ is included in Figure 1 in order to draw attention to the fact that some intermolecular V···V distances within the layers fall short of the intramolecular ones. In all these structures, the intra-trovacene geometrical parameters are inconspicuous, and therefore, only atomic distances for the spacers and selected inter-vanadium distances are listed. Slight bending of oligoalkyne chains is quite familiar;[3,7] it is too small, however, to significantly reduce π-orbital overlap of neighboring alkyne units.

Redox Properties. Compounds **4**$^\bullet$, **6**$^{\bullet\bullet}$, **7**$^{\bullet\bullet}$, and **8**$^{\bullet\bullet}$ were subjected to cyclic voltammetry; the respective traces are depicted in Figure 2, electrochemical data being collected in the caption. Compared to parent trovacene, $E_{1/2}(\mathbf{1}^\bullet, 1+/0) = 0.26$ V versus SCE, the corresponding potentials for the derivatives **4**$^\bullet$, **6**$^{\bullet\bullet}$, **7**$^{\bullet\bullet}$, and **8**$^{\bullet\bullet}$ experience anodic shifts. This reflects the electron withdrawing nature of the alkynyl group. Differences in potentials for sequential oxidations of the

(8) (a) Schlögl, K.; Steyrer, W. *J. Organomet. Chem*. **1966**, *6*, 399. (b) Bunel, E. E.; Valle, L.; Jones, N. L.; Carroll, J. P.; Gonzales, M.; Munoz, N.; Manriques, J. M. *Organometallics* **1988**, *7*, 789. (c) Yuan, Z.; Stringer, G.; Jobe, I. R.; Kreller, D.; Scott, K.; Koch, L.; Tayler, N. J.; Marder, T. B. *J. Organomet. Chem*. **1993**, *452*, 115.
(9) (a) Kramer, J.; Hendrickson, D. N. *Inorg. Chem*. **1980**, *19*, 3330. (b) Shapiro, A. B.; Goldfield, M. G.; Rosantzev, E. G. *Tetrahedron Lett*. **1973**, 2183. (c) Levanda, C.; Bechgaard, K.; Cowan, D. O. *J. Org. Chem.* **1976**, *41*, 2700.
(10) Forbes, M. D. E.; Ball, J. D.; Avdievich, N. I. *J. Am. Chem. Soc*. **1996**, *118*, 4707.

Scheme 1

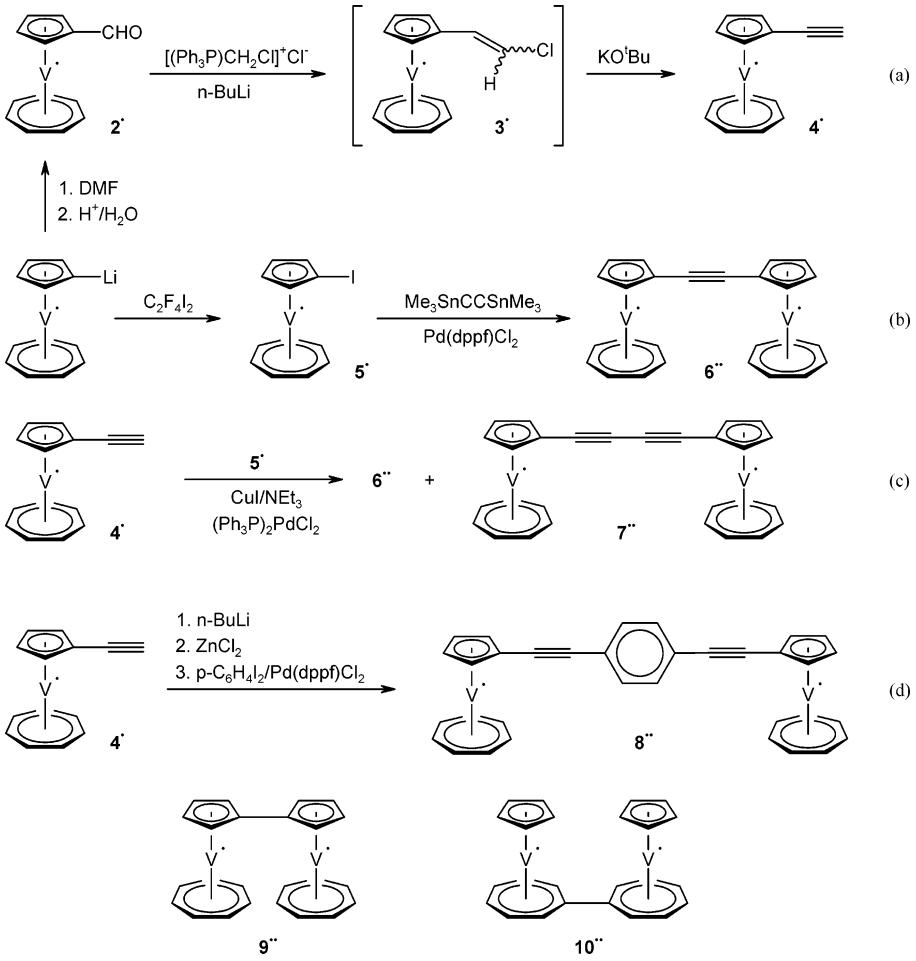

dinuclear complexes **6**••−**8**•• ("redox splitting") are unresolved, i.e., $\delta E_{1/2} \lesssim 60$ mV. This contrasts with oxidation of the ferrocene analogues Fc—$(C{\equiv}C)_{1,2}$—Fc, for which the redox splittings $\delta E_{1/2} = 130$ mV ($n = 1$) and ≈100 mV ($n = 2$) have been reported.[9c,11] Less extensive electronic coupling between the unsymmetrical sandwich units in [5]TVC—$(C{\equiv}C)_{1,2}$—[5]TVC (**6**••, **7**••) may be traced to the fact that covalency of the metal-π-perimeter bond increases with increasing ring size.[12] Therefore, the bridge η^5-C_5H_4—$(C{\equiv}C)_n$—η^5-C_5H_4 mediates less effectively in [5]TVC—$(C{\equiv}C)_{1,2}$—[5]TVC than in Fc—$(C{\equiv}C)_{1,2}$—Fc because in the former metal−ligand bonding is dominated by the (η^7-C_7H_7)V fragment which is not connected to the spacer.[13] It should be mentioned that the dependence of the magnitude of $\delta E_{1/2}$ on the site of connection in bitrovacenes has been established recently for the case of the two linkage isomers (η^7-C_7H_7)V(η^5-C_5H_4—η^5-C_5H_4)V(η^7-C_7H_7) (**9**••) and (η^5-C_5H_5)V(η^7-C_7H_6—η^7-C_7H_6)V(η^5-C_5H_5) (**10**••). Accordingly, the values are as follows: $\delta E_{1/2}$(**9**••, 2+/1+, 1+/0) = 140 mV, $\delta E_{1/2}$(**9**••, 0/1−, 1−/2−) = 220 mV;[14a] $\delta E_{1/2}$(**10**••, 2+/+, +/0) = 160 mV, $\delta E_{1/2}$(**10**••, 0/1−, 1−/2−) = 330 mV.[14b] As is generally observed for trovacene derivatives, the waves for reversible primary oxidation of **6**••, **7**••, and **8**•• are followed by irreversible secondary and tertiary oxidation at more positive potentials.

A more diversified picture is encountered for the reductions. Only **6**•• is "well-behaved" in that two reversible one-electron waves are seen which display the redox splitting $\delta E_{1/2}$(**6**••, 0/1−, 1−/2−) = 150 mV. The larger magnitude of $\delta E_{1/2}$ for reductions compared to oxidations which involve the same redox orbital is a common phenomenon and has been commented on previously.[14] Reduction of **7**•• seems to be initiated by an irreversible reduction, most likely of the spacer. This may occur because the more extended π-electron system features a lower lying LUMO which is now populated in preference to the central metal atoms V^0. A broad wave follows at more negative potentials which shows signs of resolution into two close lying one-electron processes; it

(11) Redox splitting $\delta E_{1/2}$ values are subject to medium effects: Barrière, F.; Camire, N.; Geiger, W. E.; Mueller-Westerhoff, U. T.; Sanders, R. *J. Am. Chem. Soc.* **2002**, *124*, 7262. Yet, the anions BF_4^- (ref 10) and ClO_4^- (this work) are sufficiently similar to warrant comparison of the $\delta E_{1/2}$ values obtained.

(12) (a) Fischer, R. D. *Theor. Chim. Acta* **1963**, *1*, 418. (b) Rayón, V. M.; Frenking, G. *Organometallics* **2003**, *22*, 3304.

(13) Note the distinction between the designations "bridge" and "spacer": whereas the bridge encompasses the complete organic unit connecting the central metal atoms in a dinuclear complex, the spacer separates the metallocenyl building blocks and therefore does not include the η^n-π-perimeters. For further elaboration of the relevance of this point see: Launay, J. P. *Chem. Soc. Rev.* **2001**, *30*, 386.

(14) (a) Elschenbroich, Ch.; Schiemann, O.; Burghaus, O.; Harms, K.; Pebler, J. *Organometallics* **1999**, *18*, 3273. (b) Elschenbroich, Ch.; Plackmeyer, J.; Harms, K.; Burghaus, O.; Pebler, J. *Organometallics* **2003**, *22*, 3367.

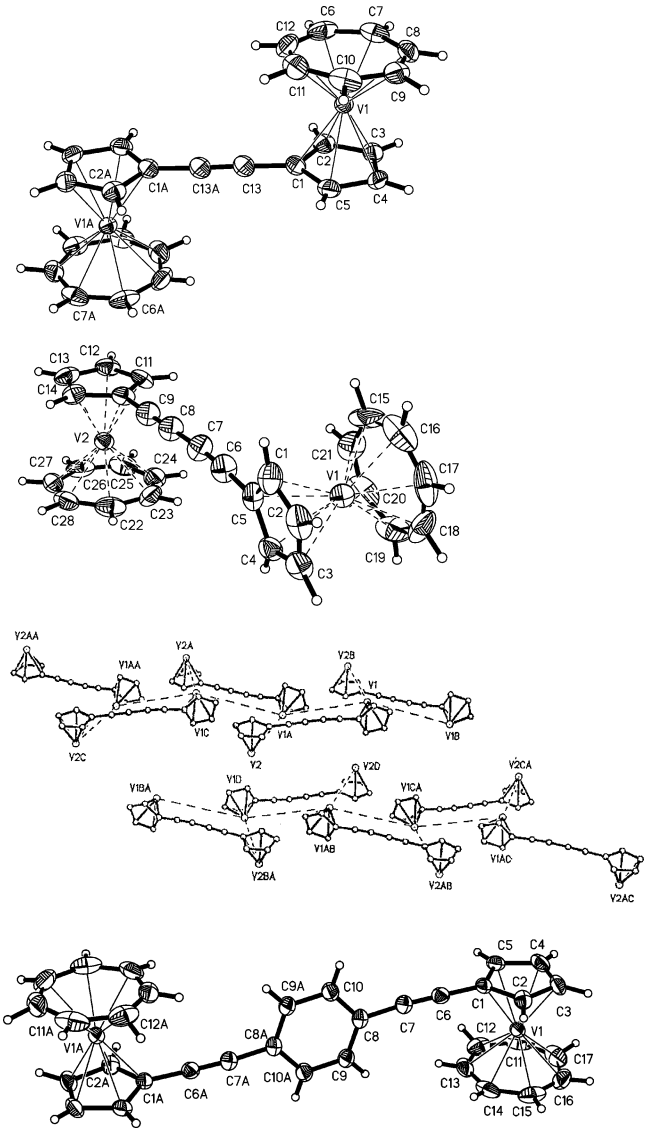

Figure 1. ORTEP drawings of the di([5]trovacenyls, **6••**, **7••**, and **8••** (50% probability) and packing diagram for **7••** (the tropylium rings have been deleted for clarity). Selected bond distances (Å) and angles (deg): for **6••** C(1)−C(13) 1.424(3), C(13)−C(13A) 1.206(4), C(1)−C(Cp) mean 2.264(2), V(1)−C(Tr) mean 2.182(2), C−C(Cp) mean 1.414(1), C−C(Tr) mean 1.404(1), V(1)−Cp centr 1.9183(11), V(1)−Tr centr 1.4645(9), V(1)···V(1A) 7.602(1), angle between the two sandwich axes 180.0; for **7••** C(5)−C(6) 1.437(11), C(6)−C(7) 1.202(11), C(7)−C(8) 1.368(12), C(8)−C(9) 1.205(11), C(9)−C(10) 1.419(11), C(5)−C(6)−C(7) 177.5(10), C(8)−C(9)−C(10) 178.6(9), angle between the two sandwich axes 98.9, V(1)···V(2) 9.432(1), V(1)···V(1B) 6.6790(17), V(2)···V(1a) 6.9606(19); for **8••** C(1)−C(6) 1.427(4), C(6)−C(7) 1.198(4), C(7)−C(8) 1.442(4), C(8)−C(9) 1.383(5), C(8)−C(10) 1.402(5), C(9)−C(10A) 1.388(5), C(10)−C(9A) 1.388(5), V(1)···V(1A) 17.27(5), angle between the two sandwich axes 180.0, phenylene−Cp 97.1.

would have to be assigned to sequential central metal reduction steps. A more complicated and at present uninterpretable CV response is observed in the strongly cathodic region for **8••**.

EPR Spectroscopy. Electro- and magnetocommunication are complementary in that the former reflects the degree of charge delocalization while the latter depends on spin delocalization and/or spin polarization. Nonetheless, both phenomena represent different facets of donor/acceptor interactions, and it is therefore legitimate to search for parallel

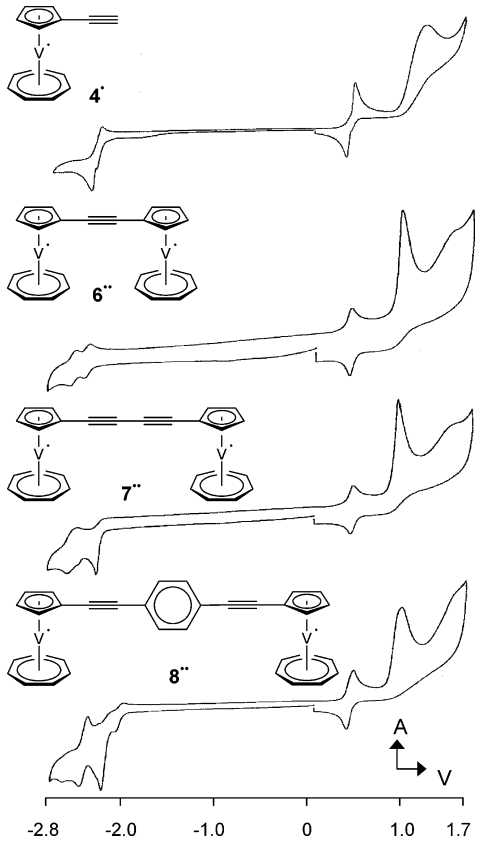

Figure 2. Cyclic voltammograms of the complexes **4•**, **6••**, **7••**, and **8••** in DME/0.1 M Bu_4NClO_4 at −35 °C and ν = 100 mV/s vs SCE. **4•**: $E_{1/2}(+, 0) = 0.39$ V, $\Delta E_p = 85$ mV; $E_{1/2}(0, 1-) = -2.40$ V, $\Delta E_p = 108$ mV. **6••**: $E_{1/2}(2+, 0) = 0.37$ V, $\Delta E_p = 71$ mV; $E_{1/2}(0, -) = -2.37$ V, $\Delta E_p = 68$ mV; $E_{1/2}(1-, 2-) = -2.52$ V, $\Delta E_p = 69$ mV. Redox splitting $\delta E_{1/2}(0, 1-; 1-, 2-) = 150$ mV. **7••**: $E_{1/2}(2+, 0) = 0.41$ V, $\Delta E_p = 67$ mV; $E_{pc,1} = -2.31$ V, $E_{pc,2} = -2.48$ V, $E_{pc,3} = -2.58$ V. **8••**: $E_{1/2}(2+, 0) = 0.40$ V, $\Delta E_p = 90$ mV; in the cathodic regime, analysis and assignments are precarious.

trends. EPR spectra of the biradicals **6••**, **7••**, and **8••** are depicted in Figure 3, and the exchange coupling constants $|J|$, determined via simulation of the ^{51}V hyperfine patterns, amount to (−)0.92 cm^{-1} (**6••**), (−)0.56 cm^{-1} (**7••**), and (−)0.005 cm^{-1} (**8••**). The negative sign, which implies the antiferromagnetic nature of the interaction, derives from magnetic susceptometry (Figure 4).

The EPR spectra of **6••** and **7••** approach the strong exchange limit $J \gg a(^{51}\text{V})$ in that 15 lines separated by $(a^{51}\text{V})/2$ are seen which deviate to different extents from the binomial intensity distribution expected for coupling to two equivalent nuclei ^{51}V. These variations reflect the respective J values. The spectrum of **8••**, on the other hand, bears resemblance to none of the limiting cases $J \gg a(^{51}\text{V})$ and $J = 0$; rather, as the simulation shows, the case J [0.005 cm^{-1}] $\approx a(^{51}\text{V})$ [0.0065 cm^{-1}] is encountered. In this situation, hyperfine coupling significantly mixes the $m_s = 0$ singlet and triplet wave functions where m_s is the eigenvalue of S_z. As a result, transitions between both $m_s = 0$ levels and the triplet $m_s = \pm 1$ levels become allowed.[15] One of the $m_s = 0$ levels is primarily of triplet origin, giving rise to the principal EPR transition. The other $m_s = 0$ level is mainly of singlet vintage, contaminated by some triplet character which renders "S → T transitions" weakly allowed. In the

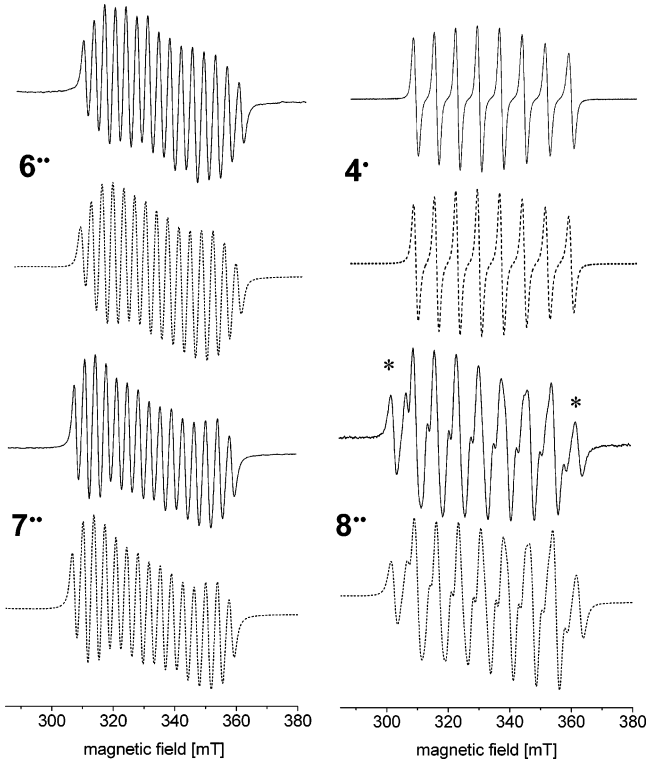

Figure 3. EPR spectra (X-band, toluene, 295 K) of mono- and dinuclear derivatives of trovacene, TVC (**1•**), and their simulated traces. [5]TVC−C≡CH (**4•**): $g = 1.981$, $a(^{51}V) = (-)7.31$ mT. [5]TVC−C≡C−[5]TVC (**6••**): $g = 1.984$, $a(^{51}V) = (-)7.28$ mT, $J = (-)\ 0.92$ cm^{-1}. [5]TVC−(C≡C)$_2$−[5]TVC (**7••**): $g = 1.985$, $a(^{51}V) = (-)7.27$ mT, $J = (-)0.56$ cm^{-1}. [5]TVC−C≡C−C$_6$H$_4$−C≡C-[5]TVC (**8••**): $g = 1.987$, $a(^{51}V) = (-)7.27$ mT, $J = (-)0.005$ cm^{-1}.

EPR spectrum of a biradical, S → T transitions appear as sidebands which are separated by $2J$.[16] Therefore, if the singlet resonances are identified as such, the quantity J may directly be read off the EPR spectrum. Applied to the spectrum of the dinuclear complex **8••**, the singlet resonances marked by asterisks are the low-field and high-field components of octets stemming from ^{51}V hyperfine coupling. Therefore, from their distance (600 G) the amount $7a(^{51}V)$ (490 G) must be subtracted to yield $2J$ (110 G). It is gratifying to note that the value $J = 55$ G (0.005 cm^{-1}) inferred from the positions of the singlet resonances of **8••** is in perfect agreement with the result from spectral simulation.

For the discussion of the effect which ethynyl groups in the spacer exert on the extent of magnetic interaction, knowledge of J for spacer-free [5-5]bitrovacene (**9••**) is desirable. However, the strength of exchange coupling in this case precludes quantification by means of fluid solution EPR spectroscopy, and only a lower limit, $|J| \geq 1.5$ cm^{-1}, can be given. The value J(**9••**) = −2.78 cm^{-1} obtained from magnetic susceptometry in the solid state (vide infra) is not strictly comparable with the fluid solution EPR data for **6••**−**8••** since it represents a maximum value characteristic for the *trans*-conformation, established by X-ray crystallography. J(**9••**) in fluid solution is expected to be considerably smaller, because conformations with impaired conjugation between the two cyclopentadienyl rings will be adopted. Notwithstanding, the gradation J(**9••**) > J(**6••**) > J(**7••**) > J(**8••**) reveals that for the species [5]TVC−(C≡C)$_n$−[5]TVC attenuation of exchange interaction caused by the introduction of −C≡C− units is fairly small, amounting to a factor of ≈0.6 [0.92 ($n = 1$)/1.5 ($n = 0$); 0.56 ($n = 2$)/0.92 ($n = 1$)]. Since the lower limit at which exchange coupling manifests itself in the ^{51}V hyperfine pattern is $J \approx 5 \times 10^{-4}$ cm^{-1}, the attenuation factor of 0.6 per −C≡C− unit in the spacer

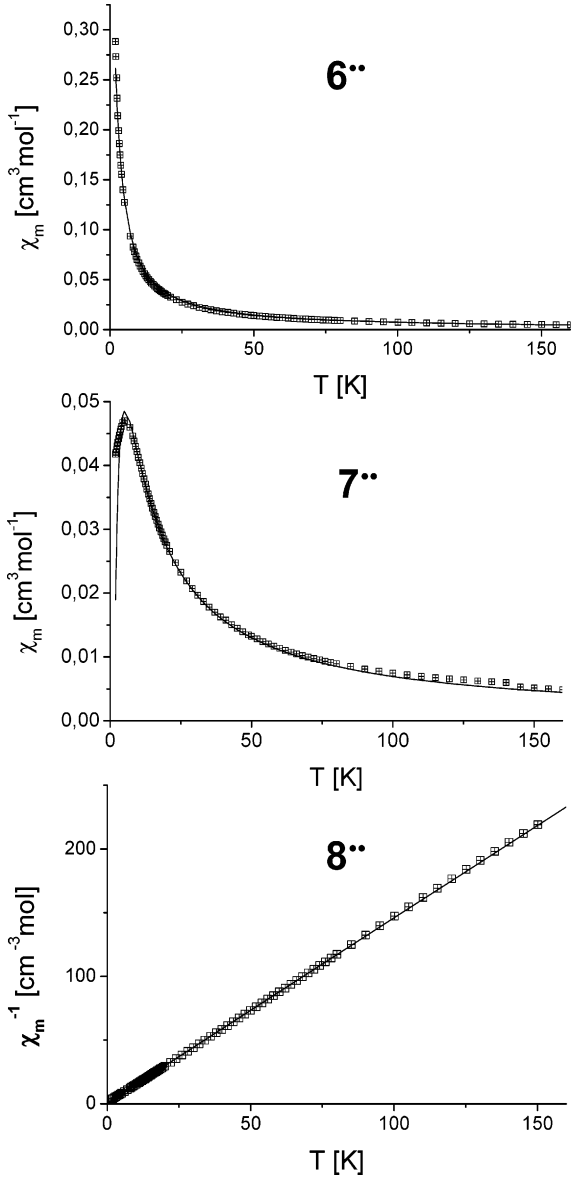

Figure 4. Temperature dependence of the magnetic susceptibility χ_m for **6••** and **7••**, of $1/\chi_m$ for **8••**, and least-squares fits according to functions given in the text. **6••**: $J = -1.45$ cm^{-1}, $\Theta_w = -1.38$ K, $C = 0.73$ cm^3 K mol^{-1}. **7••**: $J = -3.84$ cm^{-1}, $\Theta = -5.12$ K. **8••**: J not accessible, $\Theta_w = -1.04$ K, $C = 0.713$ cm^3 K mol^{-1}.

(15) (a) Briere, R.; Dupeyre, R. M.; Lemaire, H.; Morat, C.; Rassat, A.; Rey, P. *Bull. Soc. Chim. Fr.* **1965**, 3290. (b) Glarum, S. H.; Marshall, J. H. *J. Chem. Phys.* **1967**, *47*, 1374. (c) Dunhill, R. H.; Symons, M. C. R. *Mol. Phys.* **1968**, *15*, 105. (d) James, P. G.; Luckhurst, G. R. *Mol. Phys.* **1970**, *18*, 141. (e) Yeter, D. Y.; Hatfield, W. E. *Inorg. Chim. Acta* **1972**, *6*, 440.

(16) Duggan, M. D.; Hendrickson, D. N. *Inorg. Chem.* **1974**, *13*, 2929. In this reference, the separation of the sidebands amounts to 4J because the Hamiltonian, treating exchange interaction, is written $\mathcal{H} = -2J\hat{S}_1\cdot\hat{S}_2$.

implies that carbon rods [5]TV̇C−(C≡C)$_n$−[5]TV̇C ($n \leq 15$) should be amenable to study by EPR. The very weak exchange coupling observed for **8••** demonstrates that introduction of a *para*-phenylene unit attenuates much more strongly than an ethynediyl unit. Nevertheless, an exchange interaction across a distance of 17 Å is discernible here. A systematic study of oligophenylene spacered [5-5]bitrovacenes therefore is underway. The small magnitude of exchange coupling at these large distances and the requirement to exclude intermolecular interactions renders EPR study in dilute fluid solution eminently suitable in this endeavor. Furthermore, the rigidity of the spacers present in **6••**−**8••** rules out direct contacts between the terminal radical centers which could arise, if the spacers were conformationally flexible. Consequently, the EPR spectra of **6••**−**8••** in fluid solution exhibit only a small temperature dependence which is of the type attributable to changes in the rate of molecular tumbling rather than of intramolecular dynamics. In the latter case, alternating line widths would be expected but fail to be seen for **6••**−**8••**. The strongly differing response of the line width pattern on temperature change for flexible and rigid biradicals has been convincingly demonstrated for the species İm−(CH$_2$)$_4$−İm and İm-(C≡C)$_2$−İm (İm = iminoxyl group).[9b] The organometallic biradicals **6••**−**8••** clearly mimick the latter.

Magnetic Susceptometry. Discrepancies between fluid solution and solid state results may be outlined for the series of spacer-containing [5-5]bitrovacenes under investigation here. Complex **8••**, which contains the extended spacer −C≡C−C$_6$H$_4$−C≡C−, meets expectation in that exchange coupling is much too small to significantly affect magnetic susceptibility χ: the plot of $1/\chi$ versus temperature yields a straight line which intersects the T axis at $\Theta_w = -1.04$ K (Figure 4). Curie−Weiss behavior of two independent unpaired electrons therefore prevails; the very small negative Weiss temperature Θ_w may be traced to minute, intermolecular, antiferromagnetic interactions. Di([5]trovacenyl)-ethyne **6••** gives rise to a χ/T plot which can be fitted to the Bleaney−Bowers function[17]

$$\chi_m = 2Ng^2\mu_B{}^2/[kT(3 + \exp(-J/kT))]$$

furnishing the value J_χ(**6••**) = −1.45 cm^{-1}. Interestingly, the attenuation factor J_χ(**6••**)/J_χ(**9••**) = 0.52, which applies to the solid state, closely resembles J_{EPR}(**6••**)/J_{EPR}(**9••**) = 0.6 for fluid solution. This is plausible in view of the fact that intercyclopentadienyl conjugation mediated by an alkynediyl spacer is conformationally independent.

The case of di([5]trovacenyl)butadiyne (**7••**) is slightly more complicated because, surprisingly, the χ/T plot suggests an antiferromagnetic interaction exceeding that observed for the shorter spacer-containing complex **6••**. The value J_χ(**7••**) = −3.84 cm^{-1} is obtained through fitting the data to the modified Bleaney−Bowers function[17]

$$\chi_m = 2Ng^2\mu_B{}^2/[k(T - \Theta)(3 + \exp(-J/kT))]$$

in which intermolecular interactions are allowed for by means of an "effective temperature" $T - \Theta$. The parameter Θ considers all secondary, intermolecular effects; the simulation yielded the values Θ(**7••**) = −5.12 K. The origin of the apparent inconsistency of J_χ(**7••**) and J_{EPR}(**7••**) is readily rationalized on the basis of the structural data discussed above. In the crystal, **7••** features several intermolecular intervanadium distances which fall short of the intramolecular one of 9.43 Å (Figure 1). Therefore, adherence to the simple Bleaney−Bowers equation is not expected, and recourse to the corrected form must be taken.

It remains to comment on the mechanism(s) of exchange coupling in the diradical complexes **6••**−**8••**. In this context, two questions should be addressed: (1) Why is the exchange coupling J so weak, even in case of the short ethynediyl spacer? (2) Why is the attenuation factor, i.e., the fractional decrease in magnitude of J per ethynediyl unit introduced, so small?

With regard to question 1, attention must be drawn to the fact that the spin-bearing metal orbitals V(d_{z^2}) are virtually orthogonal to the π-orbitals of the η^5-C$_5$H$_4$ ring, because the latter are located close to the nodal plane of the V(d_{z^2}) orbital (Figure 5a). Therefore, spin delocalization into the spacer π-orbitals and coupling to generate a singlet ground state are suppressed. Two alternative mechanisms must be considered. The first mode, a π-path, consists of spin polarization of filled cyclopentadienyl orbitals $C_{ipso}(p_\pi)$ by the electron spin residing on vanadium and subsequent propagation via overlap of $C_{ipso}(p_\pi)$ with the p_π-orbitals of the bridge. Since in the biradicals **6••**−**8••** the two vanadium centered magnetic orbitals for the reason of orthogonality effect parallel spin alignment at the C_{ipso} atom and since oligoalkyne units −(C≡C)$_n$− contain an even number of π-centers, the net effect is antiferromagnetic coupling of the two vanadium centered spins. The small magnitude of J values determined for **6••**−**8••** are plausible because two bottlenecks for spin−spin interaction exist at the V/C_{ipso} interfaces where ineffective spin polarization rather than effective spin delocalizaion via orbital overlap operates. It should be mentioned that an identical result, antiferromagnetic coupling, would be expected from superexchange caused by excited state mixing. In that case, instead of spin polarization of a filled ligand π-orbital, promotion of the vanadium centered spin to an empty antibonding ligand π-orbital would have to be assumed.

With regard to question 2, the fairly small attenuation of exchange interaction per ethyne unit added to the spacer can be traced to the rotational invariance of conjugation of the $C_{ipso}(p_\pi)$ orbitals with the bridging alkyne π-system. A much stronger response is expected for successive addition of alkene spacer units, for which conjugation crucially depends on conformational angles.

Parent trovacene **1•** according to EPR and contact shift ^{1}H NMR possesses the positive isotropic hyperfine coupling

(17) (a) Bleaney, B.; Bowers, K. D. *Proc. R. Soc. London, Ser. A* **1952**, *214*, 451. (b) Kahn, O. *Molecular Magnetism*, VCH: Weinheim, 1993; Chapter 7.

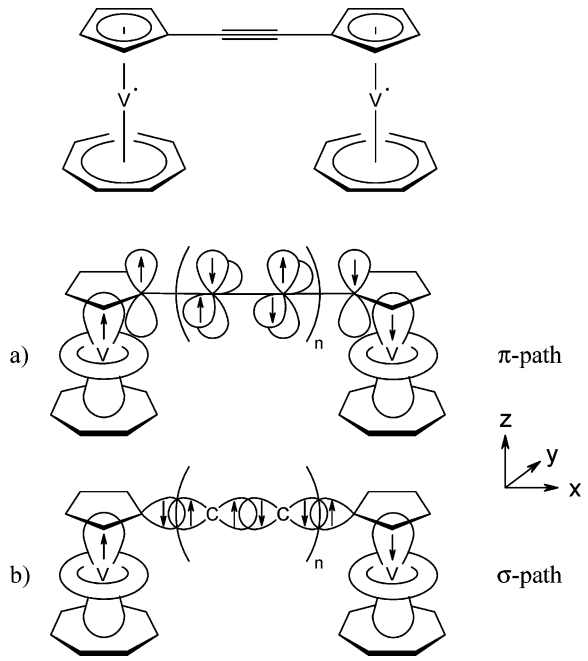

Figure 5. Exchange mechanisms in di([5]trovacenyl)oligoalkynes: (a) π-path, initiated by $V(3d_{z^2})/C_{ipso}(p_\pi)$ spin polarization; (b) σ-path, initiated by $V(3d_{z^2})-C_{ipso}(\sigma)$ spin delocalization. For di([5]trovacenyl)ethyne, di-([5]trovacenyl)butadiyne, and di-1,4-([5]trovacenylethynyl)benzene, electro- and magnetocommunication mediated by $-C\equiv C-$, $-C\equiv C-C\equiv C-$, and $-C\equiv C-C_6H_4-C\equiv C-$ spacers.

constants $a(5\ ^1H) = 1.8$ G and $a(7\ ^1H) = 4.5$ G,[18] which implies that spin density is transferred from singly occupied $V(3d_{z^2})$ to the σ-bonded protons. Therefore, a σ-path for the exchange coupling in **6••**−**8••** must also be considered (Figure 5b); its action necessitates overlap of the $V(3d_{z^2})$ orbital with the in plane a_{1g} σ-bonding orbital of the cyclic ligands. Without additional evidence, it is impossible to decide which path dominates. Important information could be gleaned from bitrovacenes which are linked via the seven-membered rings since they possess a different, known spin density at the ring protons, and from bitrovacenes which contain saturated alkane bridges and therefore have at their disposal the σ-path only.

By way of conclusion, it may be stated that in evaluations of the mediating ability of various spacers, particularly in the weak coupling regime, fluid solution EPR is vastly superior to solid state susceptometry. The study of magnetic exchange coupling across oligoalkyne units is a valuable technique in the physical characterization of these unique materials. The very nature of their molecular shape calls for techniques, however, which reliably differentiate between intra- and intermolecular effects: to this end, fluid solution EPR serves admirably.

Experimental Section

Methods and Materials. All chemical manipulations were performed with exclusion of air under dinitrogen or argon (CV) employing standard Schlenk techniques. $(C_7H_7)V(C_5H_5)$, trovacene (**1•**), was prepared from $(C_5H_5)V(CO)_4$[19a] according to the literature procedure.[19b] Dichlorobis(triphenylphosphane)palladium, dichloro-(1,1′-bis(diphenylphosphino)ferrocene)palladium, bis(trimethylstannyl)ethyne, 1,2-diiodotetrafluoroethane, and 1,4-diiodobenzene were commercial materials and were used as received. Iodo-[5]trovacene $(C_7H_7)V(C_5H_4I)$ (**5•**) was obtained from $(C_7H_7)V(C_5H_4Li)$ and $C_2F_4I_2$ as an inseparable mixture with parent trovacene and used as such.[20] Physical measurements were carried out with the following instruments: mass spectrometry, CH 7 (EI-MS), Varian MAT; cyclic voltammetry, potentiostat 552, function generator 568, multipurpose unit 563 Amel, glassy carbon working electrode, SCE reference electrode, Pt auxiliary electrode, solvent/electrolyte DME/10^{-3} M $(n\text{-Bu})_4NClO_4$, −35 °C, argon protection; EPR spectroscopy, ESP 300 (X-Band), Bruker, frequency counter TR 5214, Advantest; magnetic susceptometry, SQUID, Quantum Design. The data were corrected for magnetization of the sample holder (KLF), and diamagnetic corrections were applied to the magnetic susceptibility data based on Pascal's constants. Nonlinear least-squares-fits according to Levenberg−Marquardt[21] were performed.

X-ray Crystallography of 6••, 7••, and 8••·C_7H_8. Data were collected at 193 K on a STOE IPDS diffractometer using Mo Kα radiation. The structures were solved using direct methods and refined on F^2 values using the full matrix least-squares method, all non-hydrogen atoms anisotropic. See Table 1 for further details.

Programs used include: SHELXS-97 and SHELXL-97 (G. M. Sheldrick, University of Göttingen, Germany, 1997), STOE IPDS software (STOE & CIE GmbH., Darmstadt, Germany, 1999), SHELXTL 5.02 (Siemens Analytical X-ray Instruments Inc, Madison, WI, 1996).

(η^7-C_7H_7)V(η^5-C_5H_4CHO) (2•). *n*-Butyllithium (1.6 M in *n*-hexane, 11.8 mL, 18.9 mmol) was added at −10 °C to a solution of (η^7-C_7H_7)V(η^5-C_5H_5), **1•** (2.05 g, 9.44 mmol), in 150 mL of diethyl ether, and the mixture was stirred overnight at ambient temperature. After cooling to 0 °C, dimethyl formamide (2.9 mL, 37.8 mmol) was added, and the mixture was stirred for 30 min at 0 °C and for 1 h at ambient temperature. Hydrolysis at 0 °C with 1 mL of 2 N HCl effected a color change to dark green. After removal of the solvent in vacuo, the green residue was dissolved in toluene, the solution dried with Na_2SO_4 and filtered and the filtrate reduced to 10 mL. Separation was effected by column chromatography (Al_2O_3, 26 cm × 3 cm). First, unreacted **1•** was eluted by toluene, and then the dark green band of the product **2•** was eluted by toluene/THF (20:1). Yield: 1.03 g (4.36 mmol), 46%. EI-MS: *m*/*z* 235 (100%, M^+), 207 (14%, $\mathbf{1}^+$), 144 (4%, $M^+ - C_7H_7$), 116 (31%, $C_5H_5V^+$), 51 (34%, V^+). IR (KBr) cm^{-1}: 2771 (ν[C(O)−H]), 2718 (δ[H−C═O]), 1681, 1660 (ν[C═O]). Anal. Calcd for $C_{13}H_{12}OV$ (235.18): C, 66.38; H, 5.14%. Found: C, 65.78; H, 5.61%.

(η^7-C_7H_7)V(η^5-C_5H_4−C≡CH) (4•). *n*-Butyllithium (1.6 M in *n*-hexane, 3.42 mL, 5.47 mmol) was added dropwise at 0 °C to a solution of $[Ph_3PCH_2Cl]Cl$ (1.9 g, 5.47 mmol) in 10 mL of tetrahydrofuran (THF) leading to a deep reddish brown color of the suspension. After warming to room temperature (30 min), [5]-trovacenealdehyde **2•** (1.26 g, 5.36 mmol), dissolved in 15 mL of THF, was added over 15 min, and the solution was stirred overnight. To the greenish-brown solution, which contained a white precipitate, was added *t*-BuOK (1.23 g, 10.9 mmol), whereupon slight warming

(18) Rettig, M. F.; Stout, C. D.; Klug, A.; Farnham, P. *J. Am. Chem. Soc.* **1970**, *92*, 5100.

(19) (a) Floriani, C.; Mange, V. *Inorg. Synth*. **1991**, *28*, 263. Floriani, C. *J. Chem. Soc., Dalton Trans*. **1976**, 1046. (b) King, R. B.; Stone F. G. A. *J. Am. Chem. Soc.* **1959**, *81*, 5263.

(20) Ibrahim, B. Diploma Thesis, Marburg, 1999.

(21) Press, W. H. *Numerical Recipes*; Cambridge University Press: Cambridge, U.K., 1989.

Table 1. Crystallographic Data and Structural Refinement Details for Compounds **6••**, **7••**, and **8••**

	6••	**7••**	**8••**·C_7H_8
cryst size/mm^3	0.48 × 0.21 × 0.06	0.24 × 0.18 × 0.09	0.55 × 0.40 × 0.25
cryst syst	monoclinic	monoclinic	triclinic
space group, Z	$C2/c$, $Z = 4$	$P2_1/c$, $Z = 4$	$P\bar{1}$, $Z = 1$
unit cell	$a = 23.1727(19)$ Å	$a = 11.1333(9)$ Å	$a = 7.6621(8)$ Å
	$b = 7.9042(4)$ Å	$b = 12.3627(9)$ Å	$b = 8.0997(9)$ Å
	$c = 10.9095(9)$ Å	$c = 15.2079(10)$ Å	$c = 12.5997(16)$ Å
			$\alpha = 85.294(14)°$
	$\beta = 103.049(10)°$	$\beta = 91.260(9)°$	$\beta = 84.222(14)°$
			$\gamma = 78.708(13)°$
V	1946.6(2) Å^3	2092.7(3) Å^3	761.36(15) Å^3
cell determination	7128 reflns	7998 reflns	5000 reflns
empirical formula	$C_{26}H_{22}V_2$	$C_{28}H_{22}V_2$	$C_{41}H_{34}V_2$
fw	436.32	460.34	628.56
density (calcd)	1.489 Mg/m^3	1.461 Mg/m^3	1.371 Mg/m^3
abs coeff	0.968 mm^{-1}	0.905 mm^{-1}	0.643 mm^{-1}
$F(000)$	896	944	326
θ range	2.73−25.92°	2.12−22.49°	2.57−25.96°
index ranges	−28/28, −9/9, −13/13	−11/11, −13/13, −16/15	−9/9, −9/9, −15/15
reflns collected	7413	10892	5830
indep reflns	1893 [R(int) = 0.0271]	2696 [R(int) = 0.0934]	2313 [R(int) = 0.0680]
completeness	99.5%	98.8%	77.6%
obsd	1547 [$I > 2\sigma(I)$]	2008 [$I > 2\sigma(I)$]	1882 [$I > 2\sigma(I)$]
reflns used for refinement	1893	2696	2313
abs correction	empirical	empirical	none
T_{max} and T_{min}	0.9442 and 0.6536	0.9230 and 0.8120	
largest diff peak and hole	0.282 and −0.225 e Å^{-3}	0.823 and −0.428 e Å^{-3}	0.324 and −0.359 e Å^{-3}
treatment of hydrogen atoms	isotropic refinement	riding model	isotropic refinement
refined params	171	271	260
GOF on F^2	1.016	1.072	1.085
wR2 (all data)	0.0733	0.1958	0.1376
R1 [$I > 2\sigma(I)$]	0.0269	0.0729	0.0456

occurred, the precipitate dissolved, and the green color of the solution intensified. After refluxing overnight, more *t*-BuOK (0.61 g, 5.43 mmol) was added, and refluxing was continued. After cooling to room temperature, H_2O (20 mL) and HCl (2 N, 1 mL) were added. The aqueous phase was extracted three times with benzene, the combined organic phases were dried with Na_2SO_4, and the solvent was removed in vacuo. The residue was dissolved in 2 mL of benzene and chromatographed on Al_2O_3 (10 cm × 2 cm). The first bluish green fraction was collected and stripped from solvent, and the residue was recrystallized from a small amount (3−4 mL) of methyl cyclohexane. Cooling to 4 °C overnight yielded **4•** as an almost black fibrous material. Yield: 0.58 g (2.51 mmol), 47%. The product **2•** possesses a characteristic, nauseating smell, it is exceedingly soluble in all common organic solvents, and the solutions are very air sensitive. EI-MS: *m*/*z* 231 (100%, M^+), 153 (22%, $M^+ - 78$), 140 (36%, $M^+ - C_7H_7$), 129 (20%, $C_6H_6V^+$), 116 (8%, $C_5H_5V^+$), 51 (53%, V^+). IR (KBr) cm^{-1}: 3283 (ν[C_2−H]), 2110 (ν[C≡C]). Anal. Calcd for $C_{14}H_{12}V$ (231.19): C, 72.73; H, 5.23%. Found: C, 72.05; H, 5.40%.

(η^7-C_7H_7)V(η^5-C_5H_4I) (5•). Solutions of **1•** (0.8 g, 3.86 mmol) in diethyl ether (50 mL) and *n*-butyllithium (1.6 M, 2.41 mL, 3.86 mmol) in *n*-hexane were mixed and stirred for 6 h at room temperature. After cooling to −15 °C, a solution of 1,2-diiodo-1,1,2,2-tetrafluoroethane (0.52 mL, 3.87 mmol) in diethyl ether (6 mL) was added over 15 min. Stirring was continued for 40 min at −15 °C and for 1 h at room temperature. After hydrolysis with aqueous NH_4Cl (1 N, 0.3 mL), diethyl ether was removed in vacuo and the residue dissolved in benzene. Chromatography (40 cm × 2 cm, Al_2O_3, 8% H_2O, benzene) failed to effect separation. The product (1.04 g) consists of an approximately equimolar mixture of **1•** and **5•**, which was used as such for subsequent reactions.

(η^7-C_7H_7)V(η^5-C_5H_4−C≡C−η^5-C_5H_4)V(η^7-C_7H_7) (6••). Bis-(trimethylstannyl)acetylene (53 mg, 0.15 mmol) and iodo-[5]-trovacene **5•** (150 mg, mixture with **1•**) were dissolved in benzene (15 mL), a few milligrams of $(Ph_3P)_2PdCl_2$ were added, and the mixture was allowed to react at room temperature overnight. The color changed from violet to greenish blue. After addition of a few more milligrams of the catalyst, the mixture was refluxed for 3 h causing the color to darken considerably. Chromatography (10 cm × 2 cm, Al_2O_3/3% H_2O, toluene) after weak zones of bluish green and violet color yielded the main band (green) which, after collection, was reduced to the volume of 3 mL. After standing at 4 °C for 5 days, **6••** could be isolated as dark green rhombi. Yield: 12 mg (0.028 mmol, 18.6% referred to $Me_3SnC{\equiv}CSnMe_3$). EI-MS *m*/*z*: 436 (100%, M^+). Anal. Calcd for $C_{26}H_{22}V_2$ (436.34): C, 71.57; H, 5.08%. Found: C, 71.19; H, 5.01%.

(η^7-C_7H_7)V(η^5-C_5H_4−(C≡C)$_2$−η^5-C_5H_4)V(η^7-C_7H_7) (7••). Portions (25 mg) of CuI and $(Ph_3P)_2PdCl_2$ each in triethylamine were stirred for 10 min at 0 °C. A solution of **4•** (200 mg, 0.87 mmol) in triethylamine (15 mL) was added dropwise over 10 min, whereupon a brown precipitate formed. A solution of **5•** (230 mg, mixture with **1•**) in triethylamine (20 mL) was added, causing a color change to light green. Stirring at 0 °C was continued for 1 h followed by 10 h at room temperature and 1.5 h at reflux. The solvent was removed in vacuo and the residue dissolved in benzene (5 mL) and chromatographed (10 cm × 2 cm, Al_2O_3/2% H_2O, benzene). The first bluish gray band contained **1•**, **4•**, and **5•**; the bluish green main fraction was brought to dryness (100 mg of crude **7••**), washed with diethyl ether, and dissolved in toluene (2−3 mL). Stirring at 4 °C for one week generated a dark green, microcrystalline precipitate, which was recrystallized repeatedly from toluene until **6••** was absent according to MS analysis. Yield of **7••**: 30 mg (15%). EI-MS, *m*/*z*: 460 (100%, M^+). IR (KBr) cm^{-1}: 2219, 2149 (ν[C≡C]). Anal. Calcd for $C_{28}H_{22}V_2$ (460.36): C, 73.05; H, 4.82. Found: C, 73.18; H, 4.62.

Note: This method is not suitable for the isolation of pure **6••** because the mother liquors of the recrystallization of **7••** always contain both **6••** and **7••**.

(η^7-C_7H_7)V(η^5-C_5H_4—C≡C—C_6H_4—C≡C—η^5-C_5H_4)V(η^7-C_7H_7) (8••). *n*-Butyllithium (1.6 M, 0.27 mL, 0.43 mmol) in *n*-hexane was added at −10 °C to a solution of **4•** (0.1 g, 0.43 mmol) in THF (10 mL). After 10 min, anhydrous $ZnCl_2$ (0.43 mmol, 0.9 M solution in THF) was added and the mixture allowed to reach room temperature within 40 min. A solution of 1,4-diiodobenzene (0.085 g, 0.22 mmol) in THF (5 mL) and a few milligrams of (dppf)$PdCl_2$ were added over 10 min at room temperature, causing the mixture to turn to dark green and gradually form a green precipitate. The latter, after 2 h, was separated by filtration and washed with small amounts of THF and diethyl ether. Recrystallization from boiling toluene yielded **8••** as green needles. Yield: 100 mg (0.19 mmol, 87%). Single crystals suitable for X-ray diffraction were obtained from a saturated solution in toluene, layered with petroleum ether. EI-MS, *m*/*z*: 536 (100%, M^+). IR (KBr), cm^{-1}: 2204 (ν[C≡C]). Anal. Calcd for $C_{34}H_{26}V_2$ (536.46): C, 76.12; H, 4.89. Found: C, 75.90; H, 5.07.

Acknowledgment. This work was supported by the "VolkswagenStiftung", "Deutsche Forschungsgemeinschaft", and "Fonds der Chemischen Industrie".

Supporting Information Available: Crystallographic data (CIF format) including experimental details and complete tables of bond lengths and angles, atomic coordinates, and anisotropic displacement parameters. This material is available free of charge via the Internet at http://pubs.acs.org.

IC040090Z